

SUPPLEMENTARY DISCUSSION

Sensitivity of results to model-based interpolation. Because of the large footprint area and technical effort required by both eddy-covariance and biometric techniques, forest chronosequences typically comprise a rather limited number of stands. The age-class distribution of forest stands in the homogeneous area required by this kind of studies also imposes a limit on the sample size of the chronosequence. The inclusion of a greater number of sites, sometimes with several replicates for each age class^{9,30}, often requires to expand the footprint to a much larger area, so relaxing some of the assumptions of environmental and life-history homogeneity and resulting in a larger variability in the results, only partly related to age. Process-based and empirical models were therefore used in the present study to interpolate available C flux measurements between ages, so as to estimate C fluxes at every age in the rotation and obtain averages without the risks coming from a limited sample size. The application of models, however, albeit directly adjusted on field data, introduces the risk of artifacts related to the structure of the model itself. In order to test this possibility, mean fluxes over the rotation derived from model interpolation (as described above) were compared with the raw average of field measurements for individual stands in the chronosequence (see Supplementary Table S1). Maximum measured values of NEP were also used instead of interpolated values in the comparison with NEP_{AV} (Supplementary Fig. S3); despite the greater scatter in the results, the same linear relationship was found between maximum and mean fluxes, which amounted to about 54% of the maximum flux observed in mature stands. The negative offset in the relationship is the result of the smoothing of maxima which is implicit in model calibration. The two integration procedures also yielded consistent results on the control exerted by temperature and N deposition on average fluxes

(Supplementary Fig. S4). Also in this case, the raw average of field data resulted in a larger scatter, that can be presumably attributed to the limited number of stands in the chronosequence. Both the shape of the relationship and the value of the regression parameters, however, were only marginally affected by the integration method applied, so ruling out the possibility of an artifact in the results presented.

Effects of age and N deposition on forest NEP: individual stands vs rotation means. It is worth stressing that, when considering the 14 chronosequences for which annual NEP values for individual stands were available, these were only poorly (albeit significantly) correlated with wet N deposition at the site ($R^2 = 0.16$; Supplementary Fig. S5), as a result of the predominant effect of age on C fluxes. This is in contrast with the very good correlation observed with rotation-averaged NEP_{AV} for the same chronosequences ($R^2 = 0.92$). According to a 1-way ANOVA, time since disturbance explained 71.2% of the total variability in the dataset ($n = 83$).

Covariance with temperature, precipitation and site latitude. Additional analyses were carried out to evaluate the parallel effects of mean annual temperature, precipitation and latitude on rotation-averaged NEP_{AV} (Supplementary Fig. S6-S8). None of the variables was correlated with either N deposition or NEP_{AV} , as already discussed in the text; none of the variables was found to be statistically significant in a multiple correlation analysis, whatever the method applied. A particular attention was devoted to the possible covariate effects of temperature (Supplementary Fig. S6), through the analysis of selected sub-samples of the dataset. When only sites with low wet N deposition ($< 2 \text{ kg N ha}^{-1} \text{ yr}^{-1}$) were considered, NEP_{AV} was not significantly correlated to site mean annual temperature ($R^2 = 0.03^{ns}$). On the contrary, when only sites within a narrow range of temperatures ($8 < T < 9 \text{ }^\circ\text{C}$) were considered, NEP_{AV} was found to be significantly correlated to N wet deposition ($R^2 = 0.97^{***}$).

Figure S1

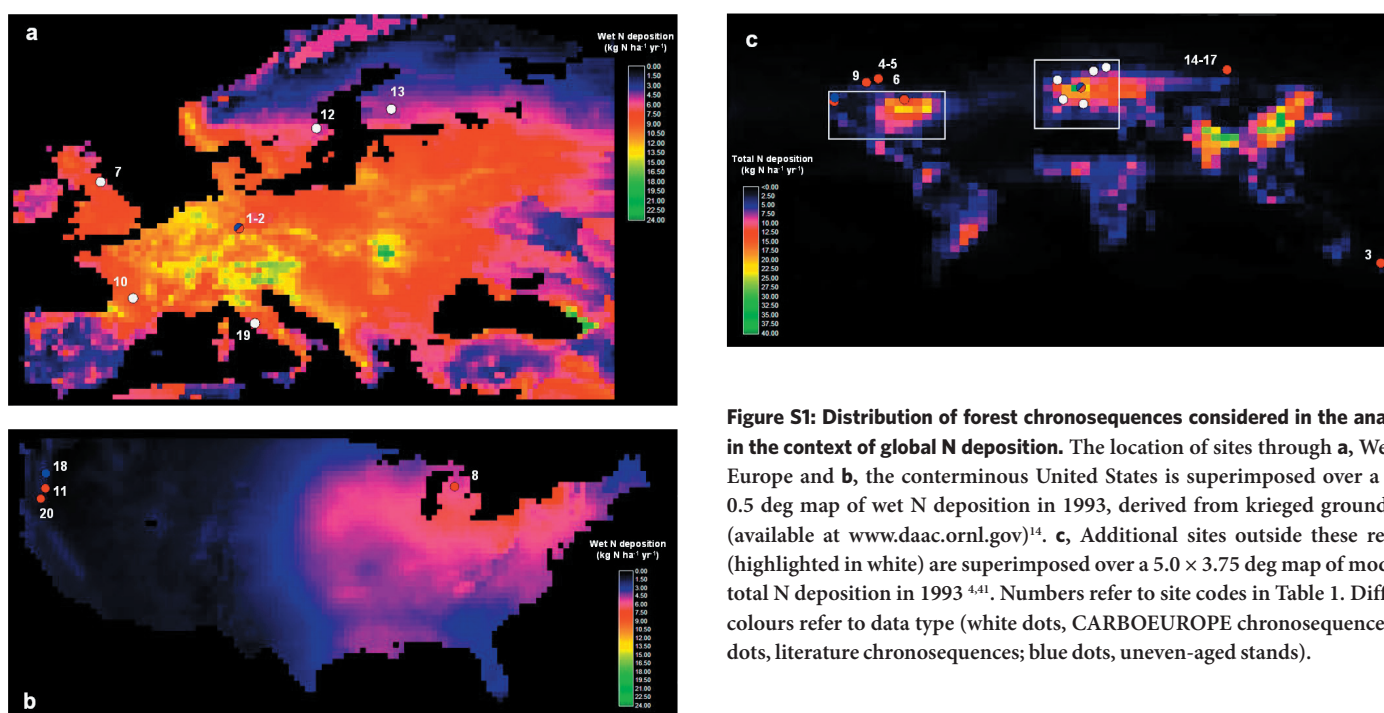


Figure S1: Distribution of forest chronosequences considered in the analysis, in the context of global N deposition. The location of sites through **a**, Western Europe and **b**, the conterminous United States is superimposed over a 0.5×0.5 deg map of wet N deposition in 1993, derived from krieged ground data (available at www.daac.ornl.gov)¹⁴. **c**, Additional sites outside these regions (highlighted in white) are superimposed over a 5.0×3.75 deg map of modelled total N deposition in 1993^{4,41}. Numbers refer to site codes in Table 1. Different colours refer to data type (white dots, CARBOEUROPE chronosequences; red dots, literature chronosequences; blue dots, uneven-aged stands).

Figure S2

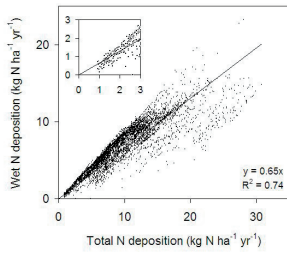


Figure S3

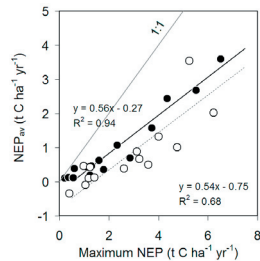


Figure S2: Relationship between wet and total N deposition. Data of wet and total N deposition across Western Europe in 1993 have been derived from the gridded 0.5×0.5 deg dataset of Holland *et al.*¹⁴ (available at www.daac.ornl.gov). A detail for low N deposition values, as commonly observed at the sites presented in Supplementary Fig. S1c, is shown in the inset.

Figure S3: Sensitivity to averaging method of the relationship between NEP_{AV} and peak NEP in mature stands. For each chronosequence, simple averages of NEP measurements in individual stands are plotted against the maximum value recorded (white circles). The results based on the interpolation of experimental data by means of process-based or empirical models (as presented in Fig. 2) are also plotted for a comparison (black dots). A linear function has been fitted by Type II regression on raw (dotted line) and interpolated values (continuous line; $n = 16$).

Figure S4

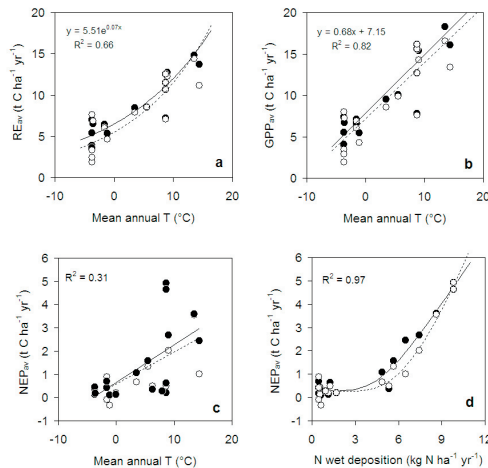


Figure S4: Sensitivity to averaging method of the analysis of environmental control on mean fluxes. C flux averages over the rotation obtained as the simple mean of measurements in individual stands (white circles and dotted regression lines) are compared with results based on data interpolation by means process or empirical models (black dots and continuous lines). **a**, Exponential relationship between average ecosystem respiration (RE_{AV}) and mean annual temperature at the study sites. **b**, Linear relationship between average ecosystem gross primary production (GPP_{AV}) and mean annual temperature at the study sites. In both panels, the only drought-prone site⁹ has been excluded from the regression. **c**, NEP_{AV} relationship with temperature and **d**, with nitrogen deposition. Coefficients of determination refer to simple averages of measured data.

Figure S5

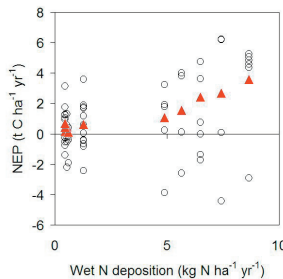


Figure S6

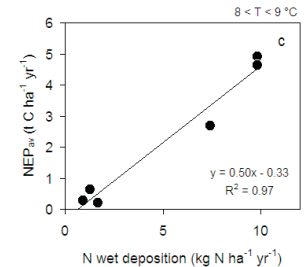
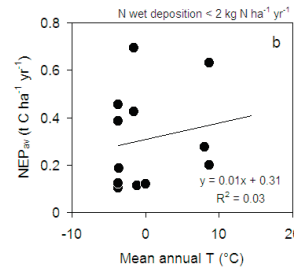
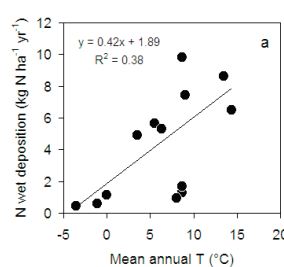


Figure S5 : Effects of age and N deposition on forest NEP: individual stands vs rotation means. Individual forest NEP values (circles) are rather poorly correlated with N depositions ($NEP = -0.09 + 0.30 \cdot N_{wet}$; $R^2 = 0.16^{***}$; $n = 83$), in contrast with rotation-averaged NEP_{AV} (red triangles; $NEP_{AV} = 0.01 + 0.35 \cdot N_{wet}$; $R^2 = 0.92^{***}$; $n = 14$). Only chronosequences with values for individual forest stands have been included in the analysis.

Figure S6: Analysis of temperature effects on NEP_{AV} . **a**, N wet deposition at the

chronosequence sites was only weakly correlated with temperature, suggesting that the covariance between the two variables plays a minor role at most in the observed relationship with NEP_{AV} . **b**, The absence of a temperature effect on NEP_{AV} is confirmed by the lack of correlation between the two variables when only sites with low levels of N wet deposition are considered (N wet deposition $< 2 \text{ kg N ha}^{-1} \text{ yr}^{-1}$). **c**, On the contrary, when only sites with annual temperatures comprised in a narrow range ($8 < T < 9 \text{ }^\circ\text{C}$) were considered, a strong correlation was observed between NEP and N wet deposition ($R^2 = 0.97^{***}$, $n = 6$).

Figure S7

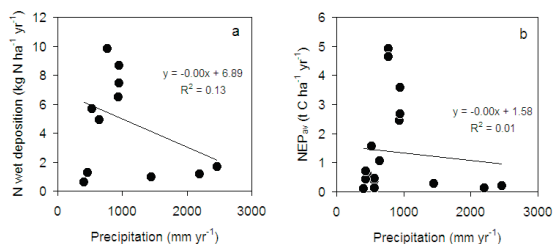


Figure S8

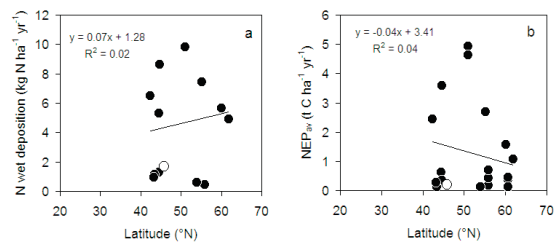


Figure S7: Analysis of precipitation effects on NEP_{AV} . **a**, N wet deposition at the chronosequence sites was only weakly correlated with annual precipitation. **b**, Lack of correlation between NEP_{AV} and annual precipitation.

Figure S8: Analysis of latitudinal changes in N deposition and NEP_{AV} . **a**, N wet

deposition at the chronosequence sites was only weakly correlated with site latitude. **b**, Lack of correlation between NEP_{AV} and site latitude. The white dot refers to the only chronosequence from the Southern Hemisphere (Site # 3 in Table 1).

Table S1: Computation of average C fluxes in forest chronosequences. Detail of data source and integration procedures used in the analysis. Average values of GPP (Raw GPP_{AV}) and NEP (Raw NEP_{AV}) over the chronosequence, obtained as the mean of raw measurements in individual stands, are presented for a comparison with averages based on model interpolation (Table 1). Also presented is the maximum NEP value measured in each chronosequence.

Table S1

Main species	#	NEP source*	NEP integration†	GPP source†	GPP integration‡	Raw GPP_{AV}	Raw NEP_{AV}	Measured max NEP	Ref.
<i>Fagus sylvatica</i>	1	EC	source	EC	source	15.6	4.9		23
	2	CF	source	NPP	source	16.1	4.6		24
<i>Nothofagus solandrii</i>	3	CF	ΔC				0.3		22
<i>Picea mariana</i>	4	CF	L03	NPP	L03	6.1	-0.1	1.1	25
	5	CF	L03	NPP	L03	6.9	0.9	3.1	25
	6	EC	L03	EC	L03	7.3	0.4	1.2	26
<i>Picea sitchensis</i>	7	EC, CF	3PG-3	EC, CF	3PG-3	14.3	2.0	6.2	¶
<i>Pinus banksiana</i>	8	CF	W02				0.5		27
	9	CF	L03	NPP	L03	4.3	-0.3	0.4	28
<i>Pinus pinaster</i>	10	EC, CF	3PG-3	EC, CF	3PG-3	16.6	3.5	5.3	¶
<i>Pinus ponderosa</i>	11	CF	L03	NPP	L03	7.6	0.5	3.6	9
<i>Pinus sylvestris</i>	12	EC, CF	3PG-3	EC, CF	3PG-3	9.9	1.3	4	¶
	13	EC, CF	3PG-3	EC, CF	3PG-3	8.5	0.7	3.2	¶
	14	CF	source	NPP	source	8.0	0.4	2.6	21
	15	CF	source	NPP	source	2.0	0.1	1.2	21
	16	CF	source	NPP	source	3.5	0.1	1.4	21
	17	CF	source	NPP	source	2.9	0.5	1.0	21
	18	CF	source	NPP	source	12.7	0.2		29
<i>Pseudotsuga menziesii</i>	18	EC, CF	3PG-3	EC, CF	3PG-3	13.4	1.0	4.8	¶
<i>Tsuga martensiana</i>	20	CF	W02				0.2		30

* EC, eddy-covariance; CF, component fluxes. † EC, eddy-covariance; CF, component fluxes; NPP, from Net Primary Production. ‡ ΔC, change in ecosystem C over the rotation; L03, empirical model in Law *et al.*⁹; 3PG-3, process model; W02, empirical model in Wirth *et al.*²¹; source, original reference.